Porcine circovirus type 2 protective epitope densely carried by chimeric papaya ringspot virus–like particles expressed in *Escherichia coli* as a cost-effective vaccine manufacture alternative

Brenda Eugenia Aguilera[1]
Gabriela Chávez-Calvillo[2]
Darwin Elizondo-Quiroga[1]
Mónica Noemí Jimenez-García[3]
Mauricio Carrillo-Tripp[3]
Laura Silva-Rosales[2]
Rodolfo Hernández-Gutiérrez[1]
Abel Gutiérrez-Ortega[1*]

[1] Unidad de Biotecnología Médica y Farmacéutica, Centro de Investigación y Asistencia en Tecnología y Diseño del Estado de Jalisco A.C., Normalistas 800, Colinas de la Normal, Guadalajara, Jalisco 44270, México

[2] Departamento de Ingeniería Genética, Centro de Investigación y de Estudios Avanzados del Instituto Politécnico Nacional, km 9.6 Libramiento Norte, Carretera Irapuato-León, Irapuato, Guanajuato 36821, México

[3] Laboratorio de la Diversidad Biomolecular, Unidad de Genómica Avanzada, Centro de Investigación y de Estudios Avanzados del Instituto Politécnico Nacional, Libramiento Norte km 9.6, Carretera Irapuato-León, Irapuato, Guanajuato 36821, México

Abstract

Porcine circovirus type 2 (PCV2) still represents a major problem to the swine industry worldwide, causing high mortality rates in infected animals. Virus-like particles (VLPs) have gained attention for vaccine development, serving both as scaffolds for epitope expression and immune response enhancers. The commercial subunit vaccines against PCV2 consist of VLPs formed by the self-assembly of PCV2 capsid protein (CP) expressed in the baculovirus vector system. In this work, a PCV2 protective epitope was inserted into three different regions of papaya ringspot virus (PRSV) CP, namely, the N- and C-termini and a predicted antigenic region located near the N-terminus. Wild-type and chimeric CPs were modeled *in silico*, expressed in *Escherichia coli*, purified, and visualized by transmission electron microscopy. This is the first report that shows the formation of chimeric VLPs using PRSV as epitope-presentation scaffold. Moreover, it was found that PCV2 epitope localization strongly influences VLP length. Also, the estimated yields of the chimeric VLPs at a small-scale level ranged between 65 and 80 mg/L of culture medium. Finally, the three chimeric VLPs induced high levels of immunoglobulin G against the PCV2 epitope in immunized BALB/c mice, suggesting that these chimeric VLPs can be used for swine immunoprophylaxis against PCV2. Volume 64, Number 3, Pages 406–414, 2017

Keywords: *capsid protein, epitope carrier, IgG response, papaya ringspot virus, porcine circovirus 2 epitope, virus-like particles*

1. Introduction

Porcine circovirus type 2 (PCV2) is responsible for many pathological conditions in swine, referred to as PCV-associated diseases [1, 2], and causes important economic losses in the swine industry worldwide. Morbidity and lethality are variable, but the usual rates are 4–30 % and 70–80%, respectively [3]. In fact, the morbidity can cause losses of 3–5 dollars per pig [4]. PCV2 capsid protein (CP) is the only structural protein of the virus. Four structural CP regions and more than five different epitopes have been described to have antigenic properties [5–7]. To this respect, a short C-terminus fragment has demonstrated to be an immunodominant linear epitope and is also part of a conformational epitope [6, 8, 9]. Commercial subunit vaccines against PCV2 consist of recombinant virus-like

Abbreviations: *CP, capsid protein; PCV2, porcine circovirus type 2; PRSV, papaya ringspot virus; VLP, virus-like particles.*

**Address for correspondence: Abel Gutiérrez-Ortega, PhD, Unidad de Biotecnología Médica y Farmacéutica, Centro de Investigación y Asistencia en Tecnología y Diseño del Estado de Jalisco A.C., Normalistas 800, Colinas de la Normal, Guadalajara, Jalisco 44270, México. Tel.: +52 3333455200, ext. 1630; e-mail: aortega@ciatej.mx.*

Received 11 December 2015; accepted 3 March 2016

DOI: 10.1002/bab.1491

Published online 20 April 2016 in Wiley Online Library (wileyonlinelibrary.com)

particles (VLPs) that result from the self-assembly of PCV2 CP. The preferred platform for the production of these PCV2 VLPs is the baculovirus expression vector system [10–12], although some works report the use of *Escherichia coli* [13] and yeast [14, 15] for such purpose.

VLPs are self-assembled macromolecular systems formed spontaneously after the expression of one or a few viral CPs. They resemble the original virus shape, size, and symmetry, but lack a genome, so they are not infectious and cannot replicate. Therefore, it is possible to induce immune responses that are as potent as those induced by a viral infection but without the associated risks [16, 17]. Uptake and processing of antigens by antigen-presenting cells are key factors in developing the cell-mediated immune response [18]. Such response depends on several antigen-associated properties, such as size, shape, surface charge, hydrophobicity, and hydrophilicity, as well as receptor interactions. Hence, VLPs are excellent inducers of the immune response, given their large and repetitive surfaces with charged, hydrophobic, and receptor-interacting properties [18].

The display of foreign amino acid sequences on the surface of plant viruses for the development of epitope vaccines has been achieved in recent times [19]. The most studied plant viruses for epitope presentation are cowpea mosaic virus [20, 21], tobacco mosaic virus [22], and papaya mosaic virus (PapMV) [23]. Potyviruses are starting to emerge in this field in spite of their high widespread in plant ecosystems. All members of the *Potyviridae* family are flexuous filamentous plant viruses, ranging from 700 to 900 nm long and 11–15 nm wide. The virion is formed with approximately 2,000 copies of the CP, each ranging from 28 to 40 kDa mass weight, depending mainly on the virus N-terminal length [24]. The potyvirus CPs possess interesting features that offer an attractive potential to their use as vaccine carriers: (i) the N- and C-termini of the potyvirus CP are exposed at the surface of virions and are highly immunogenic [25], (ii) the N-terminus varies in length and sequence depending on the virus, (iii) virus particles can be dissociated into monomers and reassembled to form virions (i.e., with encapsulated RNA) or VLPs (i.e., without RNA), and (iv) the N- and C-termini can be removed from virus particles without affecting their structure [26]. Hence, modifications in N- and C-termini of the CP might contribute to the display of attached molecules on the surface, without affecting particle formation or disrupting the core particle [25–27]. To this respect, replicative particles or VLPs from plum pox virus, Johnson grass mosaic virus, and Potato virus Y (PVY) have been evaluated as antigen and peptide presentation platforms and proved to elicit good immune responses [28–30].

In this work, the C-terminus PCV2 epitope was inserted into three different regions of the coat protein of papaya ringspot virus (PRSV) to generate chimeric particles, namely, N- and C-termini plus a predicted antigenic region located near the N-terminus. Here, we present results of the *in silico* molecular modeling, expression in *E. coli*, purification, and structural analysis by transmission electron microscopy of the wild type and the three chimeric proteins. All chimeric proteins self-assemble into VLPs of different length. This is the first report that shows the formation of chimeric VLPs using PRSV CP as an epitope scaffold. The three chimeric VLPs elicited high immunoglobulin G (IgG) levels against the PCV2 epitope in immunized BALB/c mice, as a validation of our theoretical predictions.

2. Materials and Methods

2.1. Construction of PRSV-PCV2 expression vectors

We designed two sets of primers (Table 1) to generate two PRSV-CP genes with the PCV2b-224 epitope (FNLKDPPLNP) inserted at the N- or C-termini (PRSV-PCV2-N and PRSV-PCV2-C, respectively) by sequential PCRs. We used a previously described expression plasmid as the template, which harbors the native CP gene from a PRSV isolate [31]. Simultaneously, we designed a PRSV-CP chimeric gene (PRSV-PCV2$_{19\text{-}28}$) with the insertion of the PCV2 epitope PCV2b-224 at a site of high antigenicity, according to an analysis carried out with CLC Main Workbench 6.0 (CLC Bio, Waltham, MA, USA). The PRSV-PCV2$_{19\text{-}28}$ gene was commercially synthesized (GenScript, Piscataway, NJ, USA). The three chimeric genes were designed to include an *Nco*I cleavage site, a translation start, and a glycine codon at the 5′ end plus a *Xho*I cleavage site at the 3′ end. All PCRs were performed using 200 μM dNTPs, 0.2 μM forward and reverse primers, 10–20 ng of template plasmid, and 1 U of GoTaq DNA Polymerase (Promega, Madison, WI, USA) in a 50 μL reaction. We purified the amplified final products with a MinElute PCR Purification Kit (Qiagen, Valencia, CA, USA). Subsequently, purified products and synthesized gene were digested with *Nco*I/*Xho*I enzymes (New England Biolabs, Ipswich, MA, USA), purified with a MinElute Gel Extraction Kit (Qiagen, Valencia, CA, USA), and ligated into a pET-28a(+) prokaryotic expression vector (EMD Millipore, Billerica, MA, USA), using a T4 DNA ligase (New England Biolabs, Ipswich, MA, USA). In the end, we obtained three plasmid constructs, namely, pET28-PRSV-PCV2-N, PET28-PRSV-PCV219-28, and pET28-PRSV-PCV2-C, with the PCV2 epitope insert at the PRSV CP N-terminus, high antigenicity site, or C-terminus, respectively. We confirmed the constructs by restriction pattern with *Xba*I/*Xho*I enzymes.

2.2. *In silico* prediction of PRSV wild-type and PRSV-PCV2 chimeric molecular CP structures

We built *in silico* molecular models for the wild-type and the three chimeric protein sequences following a previously reported methodology for the prediction of three-dimensional tertiary structure [32, 33]. Rosetta [34] is seemingly the best currently available method for *de novo* protein structure prediction. We used the same protocol in each case. The CP amino acid sequence was used as the initial input to generate a fragment library comprising three- and nine-residue segments of the chain through the Robetta public server [35]. This library was used locally to produce a large number of possible structures (21,000 decoys) by a Monte Carlo procedure. Such big sampling of the conformational space is several times bigger than the recommended size for *de novo* protein structure prediction in the literature. The

TABLE 1 *Primers used for inserting PCV2 epitope on PRSV CP N- and C-termini and subsequent cloning*

Primer	*Site of insertion*	*PCR round*	*Sequence (5′-3′)*
prsvpcv2N1-F	N-terminus	1	ATCCGCCATTAAATCCGAATGAAGCTGTGGATGCCG
prsvpcv2N-R	N-terminus	1 and 2	TTTTCTCGAGTCAGTTGCGCATA
prsvpcv2N2-F	N-terminus	2	TTTTCCATGGGATTCAATTTGAAAGATCCGCCATTAAATCCGAATG
prsvpcv2C1-R	C-terminus	1	GGCGGATCTTTCAAATTGAAGTTGCGCATACCCAGGA
prsvpcv2C-F	C-terminus	1 and 2	TTTTCCATGGGAAATGAAGCTGTGGATG
prsvpcv2C2-R	C-terminus	2	TTTTCTCGAGTCACGGATTTAATGGCGGATCTTTCAAATTGAA

decoy space was clustered using pairwise Cα RMSD values as a distance metric to produce a small set of models ranked by the size of the cluster they represent and an energy function that favors compact structures with well-formed secondary structure motifs (stabilized by hydrogen bonds) and buried hydrophobic residues. We selected the final model for each case by identifying the one representing the biggest cluster with the lowest Robetta energy.

2.3. Protein expression and particle purification

We transformed electrocompetent *E. coli* One Shot BL21Star (DE3) cells (Thermo Fisher Scientific, Carlsbad, CA, USA) with each plasmid. Chimeric CP expression was carried out as per Guerrero-Rodriguez et al. [31] with some modifications. Briefly, a fresh colony was taken from an LB medium agar plate, placed in 3 mL of liquid LB/kanamycin medium (50 μg/mL), and incubated overnight at 37 °C and 250 rpm. Then, 2 mL of overnight culture was transferred to a 1-L Erlenmeyer flask with 200 mL of fresh LB liquid medium and incubated at 30 °C with 250 rpm agitation. When the culture reached an OD_{600} of 1.2, expression of the recombinant protein was induced by adding 1 mM Isopropyl β-D-1-thiogalactopyranoside (IPTG) and, after 6 H, bacterial cells were collected by centrifugation at 2,370 × *g* for 15 Min at 4 °C. Cell pellets were resuspended in 1:10 of the original culture volume (20 mL) in lysis buffer (10 mM Tris, 300 mM NaCl, 10 mM ethylenediaminetetraacetic acid [EDTA], pH 7.2) and lysed by 10 rounds of 30 Sec pulses with an XL-2000 Sonicator (Misonix) at half potency. Total protein lysate was centrifuged (4 °C, 20 Min, and 2,370 × *g*), and supernatants were analyzed by SDS-PAGE and Coomassie blue staining.

We carried out immobilized metal affinity chromatography as described elsewhere [31]. Alternatively, for chimeric VLPs purification, samples were treated with 4% (w/v) polyethylene glycol (PEG) 8000 for 1.5 H at 4 °C with constant shaking and left for 1 H at room temperature (22 ± 2 °C). Afterward, the sample was centrifuged (at 4 °C, for 20 Min, at 2,370 × *g*) and the precipitate was solubilized overnight in ¼ v/v of the initial culture medium of 10 mM sodium phosphate buffer, 300 mM NaCl, 10 mM EDTA, pH 7.4. Then, samples were centrifuged (at 4 °C, for 20 Min, at 2,370 × *g*) and VLP-enriched supernatants were filtrated through a 100 kDa MWCO Amicon Ultra-4 filtration centrifugal unit (EMD Millipore, Billerica, MA, USA) following manufacturer's instructions. Samples were analyzed by SDS-PAGE Coomassie blue staining. Protein concentration was estimated with a Bradford reagent (Sigma-Aldrich, St. Louis, MO, USA).

2.4. Transmission electron microscopy of purified particles

The purified particles were adsorbed on carbon formvar coated copper grids and negatively stained with a 2% uranyl acetate solution. The observations were performed on a JEM-100C electron microscope (JEOL, Mexico City, Mexico) at an accelerating voltage of 80 kV.

2.5. Mouse immunization with PRSV chimeric particles displaying the PCV2 epitope

Twenty-four-week-old female BALB/c mice (Harlan Laboratories, Mexico City, Mexico) were divided into four groups of five individuals. Each group was immunized with 20 μg of PRSV-PCV2-N, PRSV-PCV2$_{19\text{-}28}$, PRSV-PCV2-C, or native PRSV CP (PRSV wt). All immunizations were carried out subcutaneously with 100 μL of the different preparations on days 1 and 15. Blood was collected by tail vein bleeding 1 day before immunization (bleeding 1), and 14 and 30 days after first immunization (bleedings 2 and 3, respectively). Serum samples were obtained after two consecutive incubations of collected blood (1 H at 37 °C and overnight at 4 °C) and centrifugation (10 Min at 22 ± 2 °C for 10,000 × *g*). They were preserved at –20 °C until used. Mouse care and maintenance were carried out in the Vaccine Evaluation Module of Animal Experimentation Facilities (Centro de Investigación y Asistencia en Tecnología y Diseño del Estado de Jalisco, Mexico) according to international protocols.

2.6. IgG antibody response against the PCV2 epitope

We used immune serum samples obtained from the immunization protocol to determine IgG antibody response against PCV2 epitope. For this purpose, the different VLPs (native PRSV CP or chimeric PRSV CPs) were diluted in carbonate coating buffer (10 mM sodium carbonate, pH 9.6) and coated overnight at 4 °C in a 96-well Maxisorb plate (NUNC-Thermo Fisher Scientific,

Carlsbad, CA, USA), 5 μg per well. After that, the plate was blocked with 200 μL blocking buffer (PBS, 0.05% Tween-20, 5% nonfat dry milk) for 5 H at room temperature (22 $\pm$ 2 °C) with a further three washes in washing buffer (PBS, 0.1% Tween-20). To deplete the antibodies having affinity to the PRSV CP, serum samples belonging to the same group were pooled, diluted 1:10,000 in 0.05% Tween-20, 2.5% nonfat dry milk, and preincubated with native PRSV VLPs lacking the epitope (0.3 mg/mL) 18 H at 4 °C and 5 H at room temperature (22 $\pm$ 2 °C), leaving only the antibodies that recognize the PCV2 epitope free to react with their cognate during the assay. Afterward, 100 μL of pretreated pooled sera was added to each well and plate was incubated 2 H at room temperature (22 $\pm$ 2 °C). After four washes, 100 μL of HRP-donkey anti-mouse IgG (R&D Systems, Minneapolis, MN, USA) diluted 1:1,000 in PBS, 0.05% Tween-20, 2.5% nonfat dry milk were added, and additional 1-H incubation at room temperature (22 $\pm$ 2 °C) took place. After seven washes, 100 μL of 3-3′,5-5′tetrametylbenzidine solution (Sigma-Aldrich, St. Louis, MO, USA) was added to each well and color development was stopped after 1 Min, using 100 μL of 2 N sulfuric acid solution. Finally, plates were read at 450 nm in xMark microplate absorbance spectrophotometer (Bio-Rad, Hercules, CA, USA). Each pooled sample was analyzed in duplicate. Differences between groups were analyzed by one-way analysis of variance, followed by the multiple range test using Statgraphics (Centurion XVI v16.1.11, Madrid, Spain).

3. Results and Discussion

3.1. *In silico* identification of the PRSV CP antigenic regions

In this work, we designed three chimeric PRSV CPs harboring the PCV2 epitope at different sites of the protein (Fig. 1). For simplification purposes, the chimeric PRSV CPs will be referred as follows: PRSV-PCV2-N, PRSV-PCV2-C, and PRSV-PCV2$_{19\text{-}28}$, indicating the insertion at the PRSV CP N-, C-termini, and the antigenic region, respectively. We used the method developed by Welling et al. [36], available through CLC Main Workbench 6.0 software, to find a suitable antigenic region in the coat protein of PRSV, other than the N- and C-termini, for the insertion of the PCV2 epitope. The Welling scale is based on the relative occurrence of amino acids in antigenic regions. We identified a highly antigenic region near the CP amino terminus, comprising amino acids 15–33. This antigenic region matches a glutamic acid and lysine repeat, which is accessible on the virion's surface, and for that matter on the VLPs [25, 37]. We inserted the PCV2 epitope between amino acids 18 and 19 of the native PRSV CP sequence.

3.2. PRSV CPs tertiary molecular structure

We generated the tertiary molecular structure of the wild-type and chimeric PRSV CP monomers (Fig. 2). The PRSV wt molecular tertiary structure prediction is mainly alpha, orthogonal bundle with helix hairpins (CATH classification 1.10.287). The structure correlates well with experimental data that suggest that both N-terminus and C-terminus are exposed at the surface [25]. In the chimeric proteins, the inserted epitope is also located at the CP surface. In the case of PRSV-PCV2-N and PRSV-PCV2-C, the epitope is displayed in a pocket,

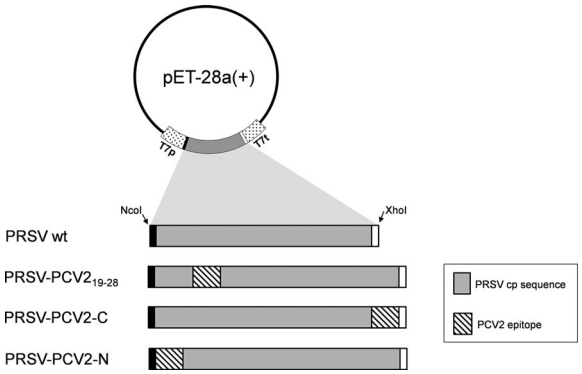

FIG. 1 *Construct design highlighting the insertion of the PCV2 epitope at different positions of the PRSV CP. The PCV2 sequence FNLKDPPLNP was inserted at a highly antigenic predicted region between amino acids 18 and 19 of PRSV CP (PRSV-PCV2$_{19\text{-}28}$), C-terminus (PRSV-PCV2-C), and N-terminus (PRSV-PCV2-N). PRSV CP wt is also included as reference. The coding sequences were cloned into bacterial expression plasmid pET28a+. T7p, T7 RNA polymerase promoter; T7t, T7 RNA polymerase terminator.*

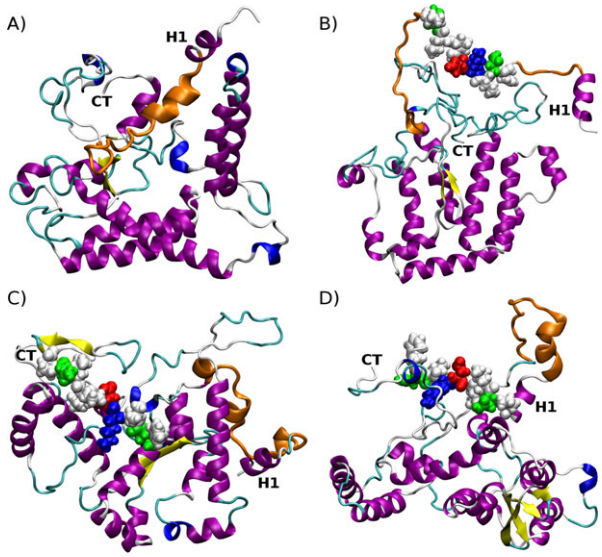

FIG. 2 *The tertiary molecular structure of the PRSV CP wt (A), PRSV-PCV2$_{19\text{-}28}$ (B), PRSV-PCV2-C (C), and PRSV-PCV2-N (D). In all cases, several features are highlighted: alpha helix motif at the N-terminus (H1), C-terminus (CT), secondary structure alpha helix (magenta) and beta sheet (yellow), glutamic acid/lysine repeat region (orange), and epitope in space filling representation for nonpolar (white), polar (green), acidic (red), or basic (blue) amino acids. Molecular visualization made with VMD.*

not surprising given that most of its amino acid composition is nonpolar in nature. On the contrary, the epitope protrudes, along with the glutamic acid/lysine repeat region, from the PRSV-PCV2$_{19\text{-}28}$ CP monomer surface. As a consequence, it should be more exposed to the solvent than its counterparts. Also, the insertion of the epitope in this region considerably disrupts the original alpha helix secondary structure of the glutamic acid/lysine repeat region. An alpha helix motif at the N-terminus, H1, is conserved in all cases. However, an alpha helix motif located at the C-terminus is conserved only in the chimeric PRSV-PCV2-C CP in comparison to the wild type. Even though all chimeric proteins retain the self-assembly structural property to some extent, as shown later, it is the PRSV-PCV2-C form that disrupts in less degree the whole wild-type tertiary structure.

3.3. Expression and purification of chimeric PRSV particles

Expression of the chimeric PRSV CPs in *E. coli* was carried out according to a previous work [31]. We analyzed the expression in IPTG-induced cultures by SDS-PAGE Coomassie blue staining. The three chimeric proteins were successfully expressed in the soluble fraction and observed as an intense band above the 31 kDa protein standard, in agreement with the expected weight of 34 kDa. Also, it can be observed that the expressed proteins have a higher mass than the native protein without epitope (Fig. 3, second lane). As demonstrated in the above-mentioned work, the native PRSV CP can be purified by immobilized metal affinity chromatography in spite of not possessing a hexahistidine tag. In agreement with this finding, the chimeric CPs reported in this work were expressed as nontagged proteins. However, analysis of the chromatography fractions revealed that none of the chimeric CPs bound to nickel-charged columns, as they are observed in the flow-through fraction before the washing step (Fig. 3). A previous hypothesis suggests that the glutamic acid–lysine repeat creates a specific environment on the VLP surface able to interact with the metal matrix [31]. Epitope insertion within or near this repeat may change the particular outside environment of the VLP, negatively affecting its affinity to the matrix. This would

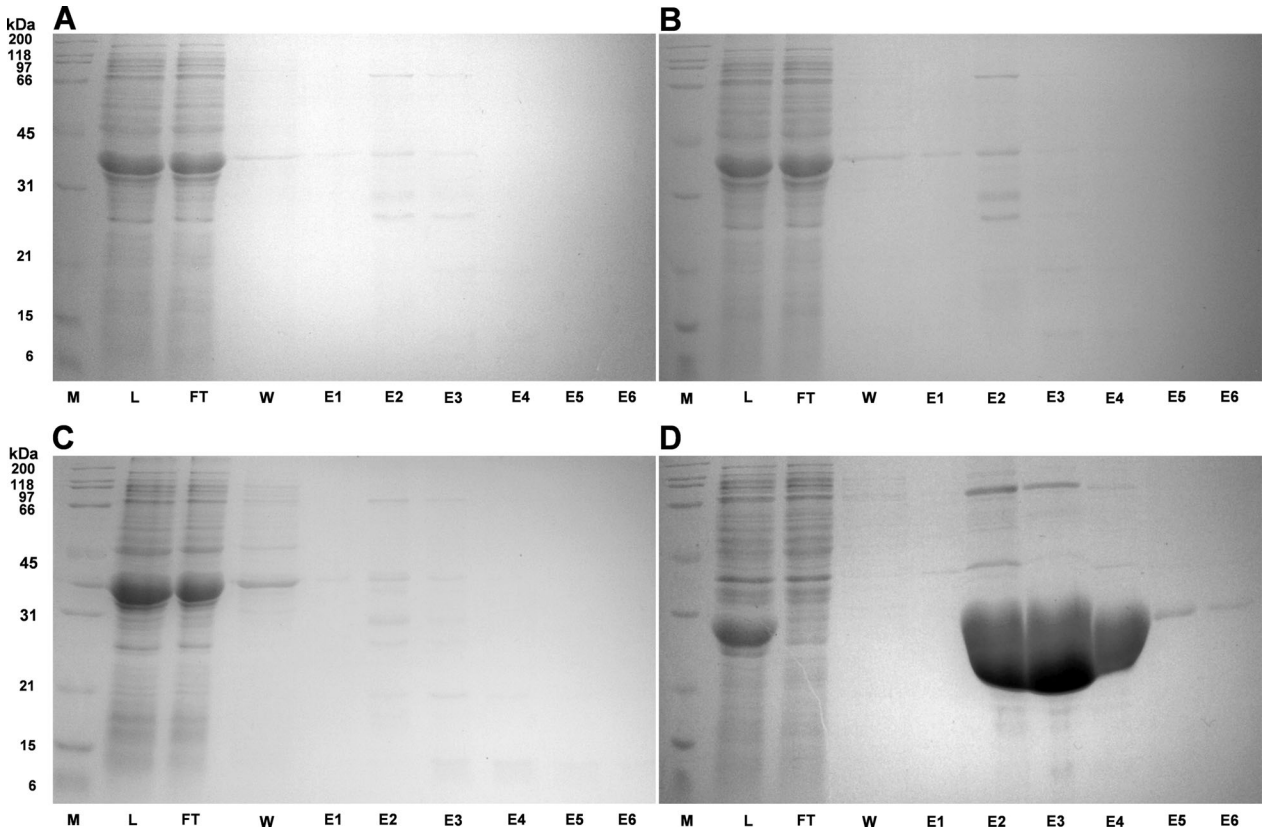

FIG. 3 *Purification of PRSV CP versions by immobilized metal affinity chromatography. (A) PRSV-PCV2-N, (B) PRSV-PCV2-C, (C) PRSV-PCV2$_{19\text{-}28}$, and (D) PRSV wt. Fractions corresponding to each step of the process were analyzed by SDS-PAGE. M, molecular weight markers; L, lysate; FT, flow through; W, washing buffer flow through; E, eluted fractions using 500 mM of imidazole.*

be the case for PRSV-PCV2-N and PRSV-PCV2$_{19\text{-}28}$. Similarly, PRSV-PCV2-C was not able to bind to the metal matrix. This observation suggests that the PRSV CP C-terminus may contribute to maintain such an external nanostructural environment for the VLP context initially defined by the interactions of the N- and C-termini at an early stage of the capsid assembly in this species of the *Potyviridae* family [26].

The chimeric PRSV particles were purified by PEG precipitation and diafiltration, as described in the Materials and Methods section. We achieved a better particle recovery, solubilizing the precipitate overnight at 4 °C. After solubilization, the particles were enriched using a 100 kDa MWCO filtration device. However, some additional purification steps, such as size exclusion chromatography, are necessary to obtain purer preparations as shown in Fig. 4. It can be observed that the chimeric version PRSV-PCV2$_{19\text{-}28}$ migrates faster than the other two, albeit they have the same theoretical mass. This can be due to an altered detergent (SDS) loading on this protein during sample denaturation as a direct consequence of the change in its tertiary structure after epitope insertion, as discussed above. This phenomenon has been reported previously for some membrane proteins [38]. The estimated yields of partially purified PRSV-PCV2-N, PRSV-PCV2$_{19\text{-}28}$, and PRSV-PCV2-C were 65, 80, and 65 mg/L of culture, respectively. These yields are comparable to those reported for other potyviral chimeric VLPs expressed in *E. coli* [29, 30]. The expression levels of PCV2 CP VLPs in insect cells using the baculovirus system reached 45 μg/10^6 cells, which is equivalent to 45 mg/L of culture medium [12]. Taking into account these yields, together with the current prices of culture media and supplements for bacterial and insect cell protein expression, we roughly estimate a threefold reduction in the production costs of PRSV-PCV2 VLPs as compared to the baculovirus-based VLPs. Previous works have reported the use of *E. coli* and *Saccharomyces cerevisiae* for the expression of PCV2 CP as an attractive alternative to the baculovirus-based system thus far employed for PCV2 vaccine production. For instance, Yin et al. [13] expressed a native PCV2 CP sequence fused to a histidine tag followed by a small ubiquitin-like modifier fusion partner at its amino terminus, using the pET28a vector, resulting in PCV2 CP VLPs after immobilized metal affinity chromatography and removal of the fusion partner with a protease. On the other side, Nainys et al. [15] demonstrated the formation of VLPs after the expression of PCV2 CP sequences from three different virus isolates in the yeast *S. cerevisiae* employing a chimeric promoter, and purification by sucrose and cesium chloride density gradient centrifugation. Notably, a recent publication by Wu et al. [39] reported the expression of a codon-optimized PCV2 CP sequence without any tag in *E. coli* using the pET24 plasmid. The PCV2 CP was purified by a one-step size exclusion chromatography protocol, yielding 50 mg/L of culture medium and, most important, also assembled into VLPs. Additionally, these VLPs stimulated the production of neutralizing antibodies in intraperitoneally immunized mice, as demonstrated by an *in vitro* assay. We find a similarity between the above-mentioned work and ours regarding the yields obtained and the small number of purification steps that were carried out, which must result in a reduction of the manufacture costs.

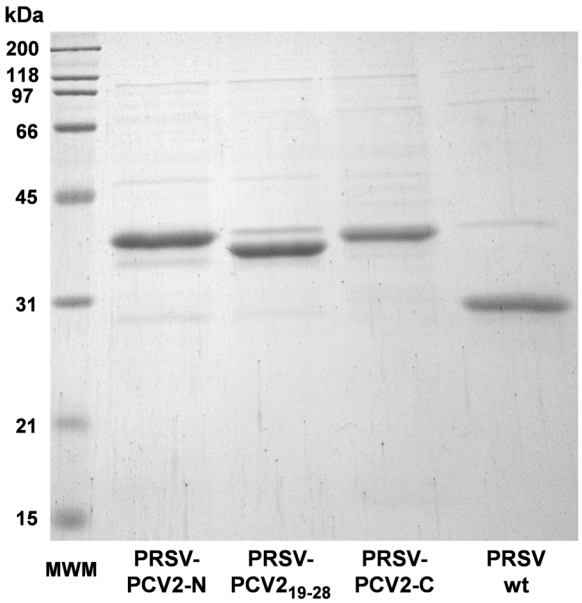

FIG. 4 *PRSV CP versions purified by 4% PEG precipitation and diafiltration and analyzed by SDS-PAGE. MWM, molecular weight marker.*

3.4. Analysis of the chimeric PRSV particles by transmission electronic microscopy

We analyzed the structure of the purified particles by transmission electron microscopy (Fig. 5). VLPs ranging from 150 to 500 nm in the PRSV-PCV2$_{19\text{-}28}$ sample were formed, while VLPs no longer than 200 nm were observed in the PRSV-PCV2-N sample. Conversely, the PRSV-PCV2-C sample presented VLPs smaller than 100 nm. Apparently, the insertion at the PRSV CP N-terminus did not impair CP assembly into rod-shaped VLPs. Nonetheless, the VLPs were far from reaching the length of chimeric PVY VLPs, expressed in *E. coli* reported by Kalnciema et al. [30], some of them larger than 2,000 nm, doubling the wild-type virion size. It is noteworthy to mention that these authors use a sophisticated strategy to avoid affecting the VLP assembly by incorporating a $(G_4S)_3$ linker between foreign and CP sequences. This method allowed the insertion of more than 70 amino acids in the CP. In our case, the insertion of 10 amino acids at the PRSV CP C-terminus affected particle assembly dramatically. It is possible that the PRSV-PCV2$_{19\text{-}28}$ insertion does not affect quaternary interactions needed to form long particles, given that it is completely outside the CP. In contrast, the other two chimeric forms have to accommodate the epitope in a pocket, producing small conformational changes, big enough to destabilize such quaternary interactions, hence rendering shorter particles, more notably in the case of the PRSV-PCV2-C form. It would be interesting to find out whether

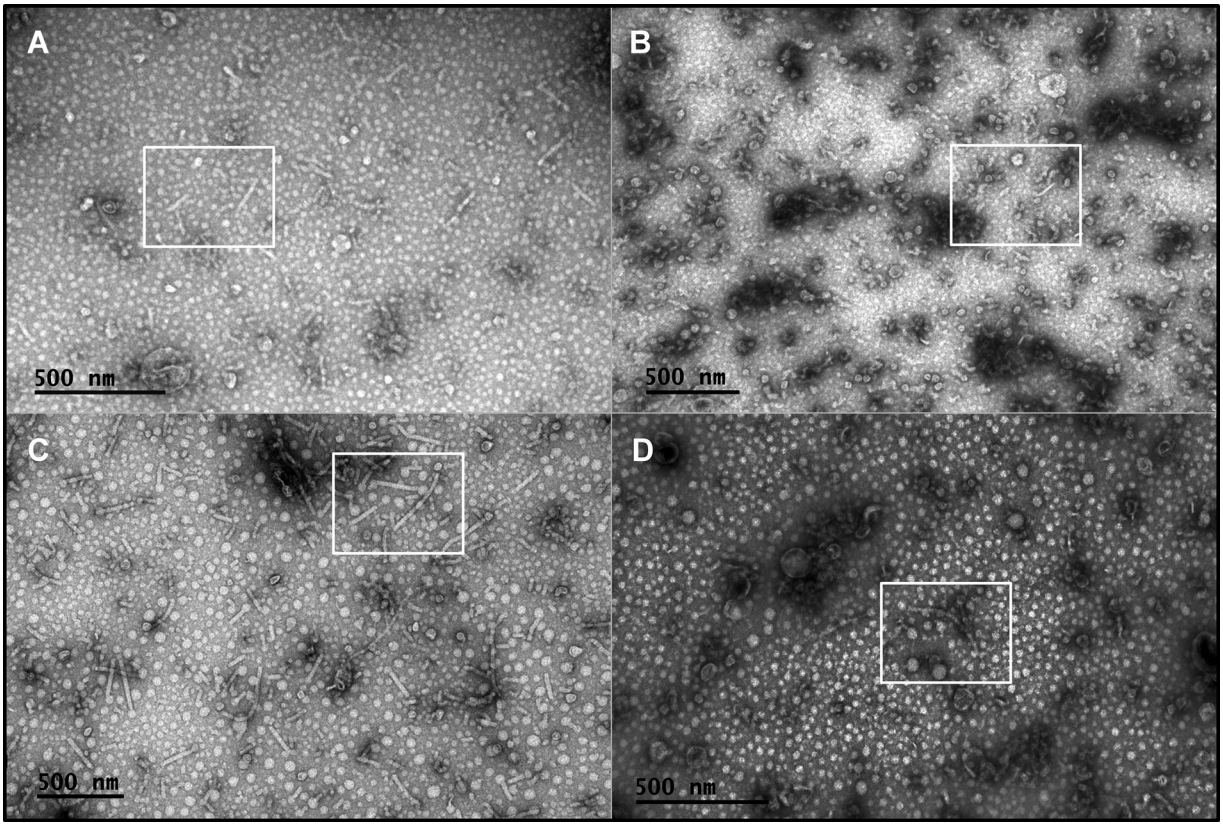

FIG. 5 *Observation of VLPs derived from PRSV CP wild-type and chimeric versions by transmission electron microscopy. (A) PRSV-PCV2-N, (B) PRSV-PCV2-C, (C) PRSV-PCV2$_{19\text{-}28}$, and (D) PRSV wt.*

VLP formation is differently affected by other sequences of the same length as the epitope inserted at the PRSV CP places reported in this work. We note that the VLP preparations, when slowly thawed in ice after being stored in 10 mM phosphate buffer, 300 mM NaCl, 10 mM EDTA, pH 7.4, for 2 months at –20 °C, did not undergo aggregation. Aggregation of native PRSV preparations after purification has been documented. At the final resuspension step, EDTA addition helps to avoid this problem [40].

3.5. Immunogenicity of chimeric PRSV particles in BALB/c mice

BALB/c mice were injected subcutaneously with the different VLP chimeric versions without any adjuvant at days 1 and 15. We determined anti-PCV2 epitope IgG levels in serum samples collected from these animals at day 30 (Fig. 6). The three chimeric versions triggered very similar IgG levels (10,000 titers), although there were statistically significant differences ($\alpha = 0.05$) between all groups; PRSV-PCV2-C induced higher IgG titers, followed by PRSV-PCV2-N and PRSV-PCV2$_{19\text{-}28}$. On the other hand, PRSV wt IgG response was negligible compared to the chimeric versions. In a recent work, the PCV2 C-terminus sequence was displayed at the surface of *cucumber mosaic virus* by genetic fusion, immunization of mice, and piglets with these chimeric particles elicited the production of antibodies against the displayed epitope and challenged pigs showed partial protection against PCV2 [41]. The mouse immunization scheme used in the mentioned work was quite similar to the one used here. However, IgG titers were not determined, so comparisons cannot be made to determine which epitope platform, cucumber mosaic virus or PRSV VLPs, triggered the best antibody response against PCV2 epitope. Nonetheless, PRSV CP VLP formation must have been crucial for inducing the IgG response, regardless of the difference in length between the chimeric PRSV VLP versions. Other works have obtained chimeric PapMV VLPs with a mean size of 100 nm. The 100 nm chimeric PapMV VLPs were strong inducers of a cytotoxic T-lymphocyte response directed to a fused influenza virus epitope [42]. PRSV CP has been evaluated previously as epitope carrier. Chatchen et al. analyzed the presentation of a 15 amino acid antigenic peptide genetically fused to the N- and C-termini of PRSV CP, proving that the C-terminus fusion enhances the antibody response to the peptide [43]. Even so, VLP formation of the chimeric CPs was not confirmed. The present work has contributed to defining whether PRSV CP fused to an epitope can self-assemble into VLPs and if particle length affects the immunogenicity of the displayed epitope. Finally, according to the high yields of *E. coli* expressed PRSV VLPs displaying the PCV2 circovirus epitope and the antibody response they elicited in

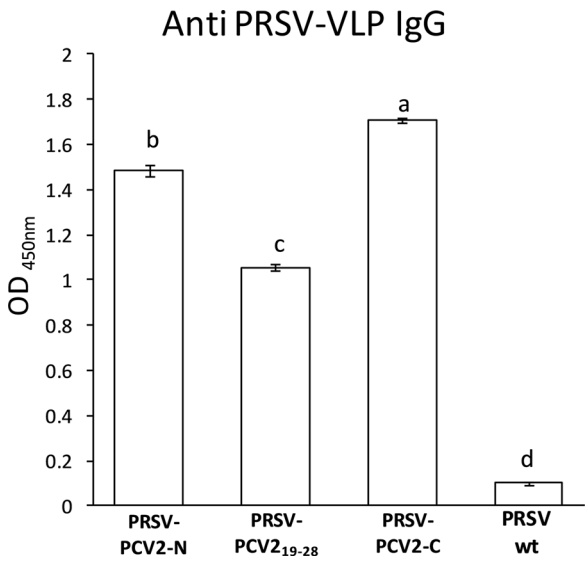

FIG. 6

IgG antibodies versus PCV2 epitope. Response in mice immunized with PRSV chimeric and wild-type versions 15 days after second immunization, where serum samples from all the groups were preincubated with excess PRSV CP wt prior to their addition to the microplate to assess the response against the epitope. Lowercase letters a–d indicate statistically significant differences between groups.

immunized mice, an experiment for assessing the protective efficacy of these VLPs against PCV2 in piglets must be carried out.

4. Conclusions

In this work, we expressed three chimeric PRSV CP versions in *E. coli* at significant yields. The proteins display a PCV2 epitope at different positions of the protein. All three chimeric proteins self-assemble into VLPs of different length in the range of 100–500 nm. Furthermore, the three chimeric VLPs induce IgG titers of 10,000 in BALB/c mice when immunized in a two-shot scheme with 20 μg of VLPs without the aid of any adjuvant. Based on our findings, we speculate that the chimeric VLPs presented here will induce high antibody protective responses in swine, perhaps mixed with a suitable adjuvant. Considering that PCV2 remains as one of the major problems in swine exploitations worldwide, the extent of the protective property of the chimeric VLPs we report here can be such that they could be a potentially cost-effective alternative to the actual baculovirus system-based PCV2 vaccine.

5. Acknowledgements

This research was supported by SEP-CONACYT (projects 83863 to A. G.-O. and 132376 to M. C.-T.). B. E. A. and G. C.-C. are indebted to CONACYT for the scholarships granted. We thank Chem. Sirenia González Pozos from Unidad de Microscopía Electrónica of Laboratorio Nacional de Servicios Experimentales, CINVESTAV, for helping us with staining and analyzing samples by TEM. We also thank Dr. Salvador Botello-Rionda (from the Centro de Investigación en Matemáticas) for allowing the use of the high-performance computing infrastructure in which the molecular modeling was performed. The authors declare no conflict of interest.

6. References

[1] Tischer, I., Mields, W., Wolff, D., Vagt, M., and Griem, W. (1986) Arch. Virol. 91, 271–276.
[2] Allan, G. M., Mc Neilly, F., Meehan, B. M., Kennedy, S., Mackie, D. P., Ellis, J. A., Clark, E. G., Espuna, E., Saubi, N., Riera, P., Bøtner, A., and Charreyre, C. E. (1999) Vet. Microbiol. 66, 115–123.
[3] Segalés, J., and Domingo, M. (2002) Vet. Q. 24, 109–124.
[4] Gillespie, J., Opriessnig, T., Meng, X. J., Pelzer, K., and Buechner-Maxwell, V. (2009) J. Vet. Intern. Med. 23, 1151–1163.
[5] Mahé, D., Blanchard, P., Truong, C., Arnauld, C., Le Cann, P., Cariolet, R., Madec, F., Albina, E., and Jestin, A. (2000) J. Gen. Virol. 81, 1815–1824.
[6] Lekcharoensuk, P., Morozov, I., Paul, P. S., Thangthumniyom, N., Wajjawalku, W., and Meng, X. J. (2004) J. Virol. 78, 8135–8145.
[7] Trible, B. R., Kerrigan, M., Crossland, N., Potter, M., Faaberg, K., Hesse, R., and Rowland, R. R. (2011) Clin. Vaccine Immunol. 18, 749–757.
[8] Truong, C., Mahe, D., Blanchard, P., Le Dimna, M., Madec, F., Jestin, A., and Albina, E. (2001) Arch. Virol. 146, 1197–1211.
[9] Shang, S. B., Jin, Y. L., Jiang, X. T., Zhou, J. Y., Zhang, X., Xing, G., He, J. L., and Yan, Y. (2009) Mol. Immunol. 46, 327–334.
[10] Kim, Y., Kim, J., Kang, K., and Lyoo, Y. S. (2002) J. Vet. Sci. 3, 19–23.
[11] Fan, H., Ju, C., Tong, T., Huang, H., and Lv, J., Chen, H. (2007) Vet. Res. Commun. 31, 487–496.
[12] Liu, Y., Zhang, Y., Yao, L., Hao, H., Fu, X., Yang, Z., and Du, E. (2015) Biotechnol. Lett. 37, 1765–1771.
[13] Yin, S., Sun, S., Yang, S., Shang, Y., Cai, X., and Liu, X. (2010) Virol. J. 7, 166.
[14] Bucarey, S. A., Noriega, J., Reyes, P., Tapia, C., Saenz, L., Zuniga, A., and Tobar, J. A. (2009) Vaccine 27, 5781–5790.
[15] Nainys, J., Lasickiene, R., Petraityte-Burneikiene, R., Dabrisius, J., Lelesius, R., Sereika, V., Zvirbliene, A., Sasnauskas, K., and Gedvilaite, A. (2014) BMC Biotechnol. 14, 100.
[16] Bachmann, M. F., and Jennings, G. T. (2010) Nat. Rev. Immunol. 10, 787–796.
[17] Pokorski, J. K., and Steinmetz, N. F. (2011) Mol. Pharm. 8, 29–43.
[18] Ahsan, F., Rivas, I. P., Khan, M. A., and Torres Suarez, A. I. (2002) J. Control. Release 79, 29–40.
[19] Plummer, E. M., and Manchester, M. (2011) Wiley Interdiscip. Rev. Nanomed. Nanobiotechnol. 3, 174–196.
[20] Brennan, F. R., Jones, T .D., and Hamilton, W. D. (2001) Mol. Biotechnol. 17, 15–26.
[21] Sainsbury, F., Canizares, M. C., and Lomonossoff, G. P. (2010) Annu. Rev. Phytopathol. 48, 437–455.
[22] Fitchen, J., Beachy, R. N., and Hein, M. B. (1995) Vaccine 13, 1051–1057.
[23] Denis, J., Majeau, N., Acosta-Ramirez, E., Savard, C., Bedard, M. C., Simard, S., Lecours, K., Bolduc, M., Pare, C., Willems, B., Shoukry, N., Tessier, P., Lacasse, P., Lamarre, A., Lapointe, R., Lopez Macias, C., and Leclerc, D. (2007) Virology 363, 59–68.
[24] W G Dougherty, A., and Carrington, J. C. (1988) Annu. Rev. Phytopathol. 26, 123–143.
[25] Shukla, D. D., Strike, P. M., Tracy, S. L., Gough, K. H., and Ward, C. W. (1988) J. Gen. Virol. 69, 1497–1508.
[26] Anindya, R., and Savithri, H. S. (2003) Virology 316, 325–336.
[27] Jagadish, M. N., Edwards, S. J., Hayden, M. B., Grusovin, J., Vandenberg, K., Schoofs, P., Hamilton, R. C., Shukla, D. D., Kalnins, H., McNamara, M., Haynes, J., Nisbet, I. T., Ward, C. W., and Pye, D. (1996) Intervirology 39, 85–92.

[28] Fernandez-Fernandez, M. R., Martinez-Torrecuadrada, J. L., Casal, J. I., and Garcia, J. A. (1998) FEBS Lett. 427, 229–235.
[29] Saini, M., and Vrati, S. (2003) J. Virol. 77, 3487–3494.
[30] Kalnciema, I., Skrastina, D., Ose, V., Pumpens, P., and Zeltins, A. (2012) Mol. Biotechnol. 52, 129–139.
[31] Guerrero-Rodriguez, J., Manuel-Cabrera, C. A., Palomino-Hermosillo, Y. A., Delgado-Guzman, P. G., Escoto-Delgadillo, M., Silva-Rosales, L., Herrera-Rodriguez, S. E., Sanchez-Hernandez, C., and Gutierrez-Ortega, A. (2014) Mol. Biotechnol. 56, 1110–1120.
[32] Bonneau, R., Strauss, C. E., Rohl, C. A., Chivian, D., Bradley, P., Malmström, L., Robertson, T., and Baker, D. (2002) J. Mol. Biol. 322, 65–78.
[33] Bonneau, R., Tsai, J., Ruczinski, I., Chivian, D., Rohl, C., Strauss, C. E., and Baker, D. (2001) Proteins 45, 119–126.
[34] Leaver-Fay, A., Tyka, M., Lewis, S. M., Lange, O. F., Thompson, J., Jacak, R., Kaufman, K., Renfrew, P. D., Smith, C. A., Sheffler, W., Davis, I. W., Cooper, S., Treuille, A., Mandell, D. J., Richter, F., Ban, Y. E., Fleishman, S. J., Corn, J. E., Kim, D. E., Lyskov, S., Berrondo, M., Mentzer, S., Popovic, Z., Havranek, J. J., Karanicolas, J., Das, R., Meiler, J., Kortemme, T., Gray, J. J., Kuhlman, B., Baker, D., and Bradley, P. (2011) Methods Enzymol. 487, 545–574.
[35] Kim, D. E., Chivian, D., and Baker, D. (2004) Nucleic Acids Res. 32, W526–W531.
[36] Welling, G. W., Weijer, W. J., van der Zee, R., and Welling-Wester, S. (1985) FEBS Lett. 188, 215–218.
[37] Silva-Rosales, L., Becerra-Leor, N., Ruiz-Castro, S., Teliz-Ortiz, D., and Noa-Carrazana, J. C. (2000) Arch. Virol. 145, 835–843.
[38] Rath, A., Glibowicka, M., Nadeau, V. G., Chen, G., and Deber, C. M. (2009) Proc. Natl. Acad. Sci. USA 106, 1760–1765.
[39] Wu, P. C., Chen, T. Y., Chi, J. N., Chien, M. S., and Huang, C. (2016) J. Biotechnol. 220, 78–85.
[40] Gonsalves, D., and Ishii, M. (1980) Phytopathology 70, 1028–1032.
[41] Gellert, A., Salanki, K., Tombacz, K., Tuboly, T., and Balazs, E. (2012) PLoS ONE 7, e52688.
[42] Babin, C., Majeau, N., and Leclerc, D. (2013) J. Nanobiotechnol. 11, 10.
[43] Chatchen, S., Juricek, M., Rueda, P., and Kertbundit, S. (2006) J. Biochem. Mol. Biol. 39, 16–21.